Climate Dynamics (2023) 61:507–518
https://doi.org/10.1007/s00382-022-06584-8

Nonidentical mechanisms behind the North Pacific summer Blob events in the Satellite Era

Yusen Liu[1] · Cheng Sun[1] · Jianping Li[2,3]

Received: 8 August 2022 / Accepted: 3 November 2022 / Published online: 23 November 2022

Abstract
The unprecedented North Pacific marine heatwave (known as the Blob) in 2013/14 winter has attracted many research interests, considering its dramatic impacts on the ecosystem and regional climate. Meanwhile, the summertime Blob events have also emerged in recent decades. In this study, we identified four Blob events in the summer of 2014, 2015, 2019, and 2020 during the Satellite Era. Here we show diversity existed in the formation of summer Blob events. The atmospheric forcing responsible for the Blob is the weakened North Pacific subtropical high (NPSH), which contributes significantly to the Blob in 2019 via anomalous shortwave radiation. However, the atmospheric forcing alone cannot fully explain all the Blob events, especially the one in 2020 when the weakened NPSH is absent. Other than the weakened NPSH, the preceding spring sea surface temperature (SST) warm anomalies in the northeast Pacific can persist into the following summer due to anomalous mixed layer heat content and significantly contribute to the Blob. A binary linear regression model considering both the SST persistence and the NPSH is constructed, successfully reproducing the observed Blob variation for the period 1982–2020 ($r = 0.76$, $p < 0.001$). The model improves the ability to capture the warm peaks in all four summer Blob events, which either single factor cannot fully depict.

Keywords North Pacific Blob · SST persistence · Atmospheric forcing

1 Introduction

Marine heatwaves in the North Pacific, named the Blob (Bond et al. 2015), refer to prolonged ocean warming events. In the winter of 2013/14, sea surface temperature (SST) in the Gulf of Alaska reached a record-breaking high anomaly (over 2℃), causing considerable damage to the local fishery and great economic loss. This extreme ocean warming event significantly impacts the coastal marine ecosystem, such as low phytoplankton biomass and harmful algal bloom (Peterson et al. 2017). Other than marine biosystem, the unprecedented influences of Blob on weather and climate also attract considerable research interest. Previous studies suggested that the Blob contributes to the anomalously cold weather in central North America and the Californian drought in 2013/14 winter (Hartmann 2015; Seager et al. 2015; Shi et al. 2021). Moreover, the Blob also plays a vital role in the extratropical-tropical and Pacific-Atlantic teleconnections. For instance, the winter Blob is closely related to the tropical Pacific SST anomalies (SSTA), which, in turn, contribute to the reemergence of Blob in the following winter (Di Lorenzo and Mantua 2016; Xu et al. 2021). It is also thought that the 2013–2014 Blob triggered the following strong El Niño in 2015/2016 (Tseng et al. 2017). In addition, the Blob is associated with the Atlantic warm pool with a one-year lead, regarded as a useful precursor (Liu et al. 2021).

The causes of winter Blob are inspected in previous studies. The persistent atmospheric ridge associated with the North Pacific Oscillation (NPO) is a direct factor contributing to the winter Blob (Amaya et al. 2016; Bond et al. 2015; Di Lorenzo and Mantua 2016). Observational and numerical model simulation results suggest that the tropical SST may play a dominant role in the formation of the winter Blob and sustain its multi-year persistence (Di Lorenzo and

✉ Cheng Sun
scheng@bnu.edu.cn

[1] College of Global Change and Earth System Science (GCESS), Beijing Normal University, Beijing, China

[2] Frontiers Science Center for Deep Ocean Multi-spheres and Earth System (FDOMES)/Key Laboratory of Physical Oceanography/Academy of the Future Ocean, Ocean University of China, Qingdao 266100, China

[3] Laoshan Laboratory, 266237 Qingdao, China

Mantua 2016). Previous studies mainly focus on the Blob events during winter. However, in 2019, strong SST anomalies were observed during the summer (JJA), referred to as Blob 2.0 (Amaya et al. 2020). The driving mechanism of summertime Blob differs significantly from the wintertime. It is suggested that the weakened North Pacific Subtropical High (NPSH) reduces the climatological westerlies, which prevents heat loss and decreases upper-level mixing in the ocean, resulting in surface/subsurface warming. Unlike the winter Blob, regional SST-cloud-shortwave radiation feedback also contributes to maintaining SST anomalies (Amaya et al. 2020). A previous study (Lee et al. 2022) has suggested that the atmosphere thermodynamic processes are vital to the increased occurrence of extreme SST warming events during the summer. The model simulation indicates that the subtropical North Pacific SST may be responsible for the anomalous atmospheric circulation that favors the Blob. The occurrence of Blob 2.0 also raises a number of studies investigating the summer Blob. In fact, summertime Blobs have occurred many times in recent years. The years 2014, 2015, 2019, and 2020 are observed to have strong SST warming events, with SSTA exceeding 1℃ (Fig. 1). It is still unclear whether these Blob events share the same driving mechanisms.

Other than the atmospheric forcing associated with the weakened NPSH, previous studies also indicate an important role of oceanic processes in maintaining the high SSTA (Tak et al. 2021). It is suggested that the anomalously low ocean salinity in the upper layer stabilizes the vertical structure, preventing further in-depth ocean mixing and intensifying the Blob (Scannell et al. 2020). The previous study also indicates that the shoaling trend in mixed layer depth (MLD) would increase the intensity of summer Blob (Amaya et al. 2021). In addition, through the seasonal changes in MLD, the anomalous SST signal in winter can be stored underneath the summer MLD and persisted till the following winter, called reemergence (Alexander et al. 1999; Deser et al. 2003). A previous study confirmed the reemergence in the evolution of SSTA during 2019–2020, highlighting the role of SSTA multi-year persistence in the Blob events (Chen et al. 2021). However, the reemergence of SSTA can not explain the summertime Blob since the warm water has been stored underneath. Also, the characteristics of large-scale SSTA persistence are seasonally dependent in the North Pacific (Namias et al. 1988). For instance, the late winter and early spring SSTA can usually persist about 3–5 months, while the summer SSTA shows a persistence barrier in September (An and Wang 2005; Bulgin et al. 2020; Ding and Li 2009; Namias and Born 1970). It is still unclear if the seasonal SSTA persistence is able to affect the summertime Blob.

In this study, we investigate the recent four summer Blob events and compare the driving mechanisms behind each of them. In addition to the simultaneous atmospheric forcing, we also highlight the importance of SSTA seasonal persistence in the northeastern Pacific on the formation of summertime Blob, which may enrich our understanding of how marine heatwaves are developed.

2 Data and method

2.1 Data

In this study, we focus on the Satellite Era since the 1980s with generally improved climate observations. SST data is derived from NOAA Extended Reconstructed Sea Surface Temperature (ERSSTv5) (Huang et al. 2017), which can be found at https://psl.noaa.gov/data/gridded/data.noaa.ersst.v5.html. The atmospheric data is derived from NCEP Atmospheric Reanalysis 2 (Kanamitsu et al. 2002) (available at https://psl.noaa.gov/data/gridded/data.ncep.reanalysis2.html). The total surface heat flux and subsurface (mixed layer depth, temperature, currents) data are derived from monthly GODAS ocean reanalysis (Behringer and Xue 2004) (available at https://psl.noaa.gov/data/gridded/data.godas.html). We also employed monthly net surface heat fluxes (longwave radiation, shortwave radiation, sensible heat flux, and latent heat flux) data from the ERA5 dataset (Hersbach et al. 2020) (available at https://cds.climate.copernicus.eu/cdsapp#!/search?text=&type=dataset).

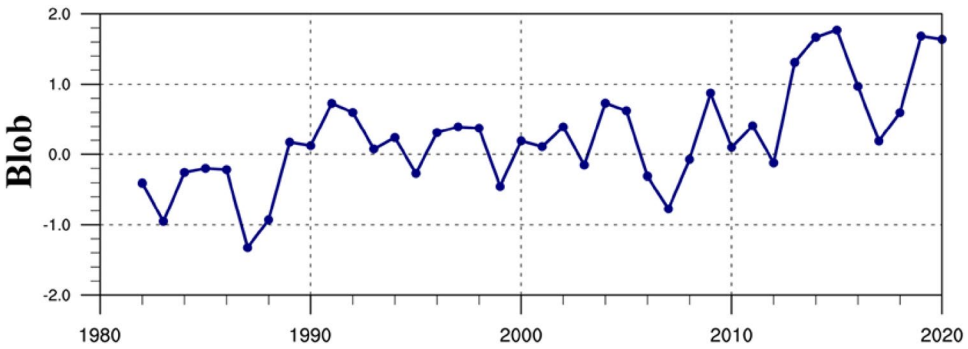

Fig. 1 The time series of the summer Blob index, which is defined as an area-weighted average of seasonal mean (JJA) anomaly of SST in the northeast Pacific (35°–50°N, 160°–130°W).

2.2 Index definitions

The Blob index is computed from the area-weighted average of SSTA over the northeastern Pacific (35°–50°N; 160°–130°W) from 1982 to 2020 (Fig. 1), generally consistent with previous studies (Amaya et al. 2021; Bond et al. 2015; Di Lorenzo and Mantua 2016). As this study focuses on the summer Blob events, the seasonal mean (June-July-August; JJA) is computed. As suggested by previous studies (Wernberg et al. 2016), marine ecosystems are often vulnerable to extreme temperature events, and the damage will emerge if the absolute value of ocean temperature anomaly meets a certain threshold. Using a regime detection method (Rodionov 2004), we find the northeastern Pacific SST exhibits two shifts in 1989 and 2013 (the figure is not shown here), corresponding to the increased occurrence of extreme SST warming events in the recent decades. Here, we define the Blob event as the SST anomaly that passes the 90th percentile (based on the reference period of 1982–2020). The SSTA in the four years (2014, 2015, 2019, and 2020) meet the criteria and are identified as the Blob events.

The NPSH index is defined the same as that used in (Amaya et al. 2020) and (Schmidt and Grise 2019). The strength of NPSH during the summer is defined by the area average in a 10° × 10° box centered on the sea level pressure (SLP) centroid (derived from JJA mean). The centroid of the NPSH is computed in agreement with that in the previous study (Amaya et al. 2020).

2.3 Mixed layer heat budget

The mixed layer heat budget in the northeast Pacific (35°–50°N, 160°–130°W) is computed based on the equation:

$$\frac{\partial T}{\partial t} = \frac{Q_{net} - Q_{pen}}{\rho c_p h_m} - \boldsymbol{U} \cdot \nabla T + R$$

$$Q_{net} = Q_{lw} + Q_{sw} + Q_{lh} + Q_{sh}$$

where ρc_p is the heat capacity of seawater, taken to be $4.088 \times 10^6 \mathrm{J°C^{-1}m^{-3}}$ and h_m is the mixed layer depth. The left-hand side of the equation indicates the temperature tendency, which is calculated by the difference in SST between August and May using the ERSSTv5 dataset. Note that the tendency term is consistent with that using the GODAS SST, which is relaxed to weekly analyzes of SST derived from the IOSST dataset. The right-hand side of the equation includes the total heat fluxes, horizontal advection, and residual terms, mainly representing the entrainment at the bottom of the mixed layer. Note that this representation allows us to capture the predominant features associated with these processes, which have been widely used in previous studies (Amaya et al. 2020; Lee et al. 2022). Each term in the equation is calculated at each grid point and averaged over the Blob region.

The net surface heat flux Q_{net} includes longwave radiation, shortwave radiation, sensible heat flux, and latent heat flux. The penetrated shortwave radiation is computed based on the equation (Paulson and Simpson 1977):

$$Q_{pen} = Q_{sw(surface)} e^{-\cdot \frac{h_m}{\xi}}$$

where ξ denotes the attenuate depth, ranging from 5 to 15 m (Zhou et al. 2015), and h_m denotes the mixed layer depth. The shortwave penetration is an intrinsic property in terms of spectral transmittance of downward irradiance in a region, which has been adjusted throughout the analysis. The sign of heat flux is adopted as positive downward (net heat input into the ocean).

3 Results

3.1 Atmospheric forcing of the blob

The NPSH is an intrinsic mode of atmospheric variability, which exhibits a considerably large explained variance in the North Pacific climate (Yun et al. 2013). Here we find that the NPSH is somewhat coherent with the summertime northeast Pacific SST on the interannual scale ($r = -0.3$, $\rho < 0.05$). In addition to the interannual variability, the NPSH also agrees with extreme SST warming events. As shown in Fig. 2, the NPSH in 2019 is the weakest during the analyzed period, corresponding to a strong Blob event in summer. This is consistent with the previous study (Amaya et al. 2020), which concluded that the weakened NSPH is a dominant factor for the Blob in 2019. In addition, the Blob events in 2014 and 2015 are also accompanied by a slightly weakened NPSH.

Here we mainly focus on the summertime (JJA mean) SSTA and SLP anomaly (SLPA) during the Blob events in 2014, 2015, 2019, and 2020 (Fig. 3). The warm anomalies during the Blob events are mainly concentrated in the northeast Pacific (35°–50°N, 160°–130°W). The core regions (SSTA > 1.8 K) are consistently located within the defining box, although the position of the 2020 Blob shifts a bit westward. The contemporary atmospheric circulations associated with SLPA are also examined during the four Blobs. In 2019, there were quite strong low-pressure anomalies in the core region of the Blob. The warm anomaly corresponds well with the weakening in the NPSH, which shifts northward to the northeast Pacific during the boreal summer. Such a low SLP anomaly is also seen in the summer of 2014, but the anomalous pressure decline is relatively weak. In

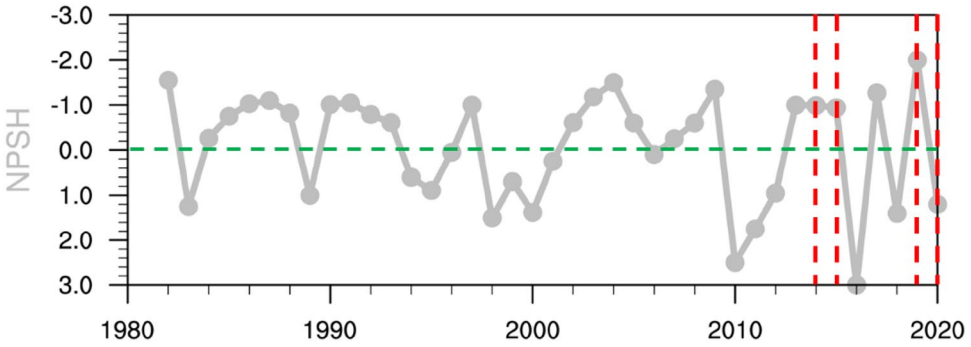

Fig. 2 The normalized time series of the summer NPSH index (1982–2020), defined as the area average in a 10° × 10° box centered on the NPSH SLP centroid (derived from JJA mean). The centroid of the NPSH is computed in agreement with that in (Amaya et al. 2020). Note that the y-axis is inverted, and the negative value indicates a weakened NPSH. The red line indicates four Blob events, and the green line indicates zero

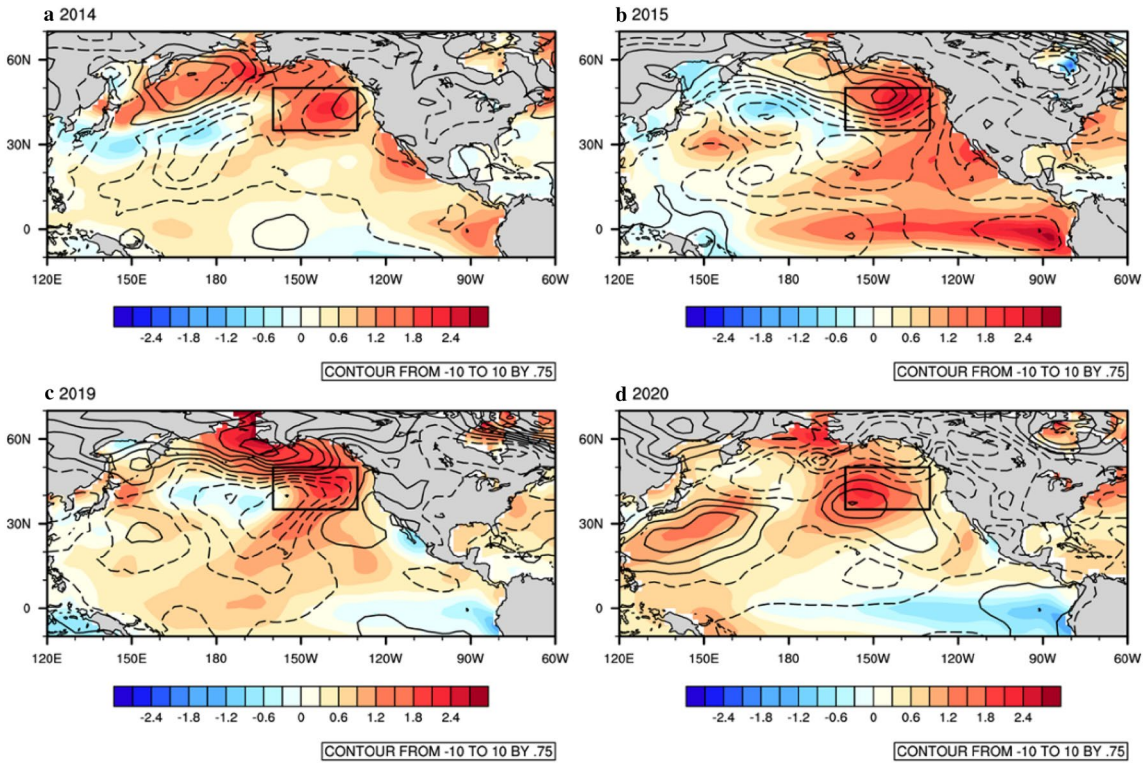

Fig. 3 The summer (JJA) SST (shading; unit: K) and SLP (contour; unit: hPa) anomalies in (**a**) 2014, (**b**) 2015, (**c**) 2019, and (**d**) 2020. Note that the negative anomalies are dashed. The black box indicates where the Blob is defined (35ºN–50ºN, 160ºW–130ºW).

2015, a weakened NPSH is also found in the North Pacific, but the anomalous center of action is located in the western North Pacific and shifts southward compared to that in 2019. The core region of SST warming is mainly governed by high anomalies, as the SLP gradients incline to the north. Whereas in 2020, the Blob is very confined to the anomalous high since the concurrent NPSH shows no weakening at all. The spatial patterns of SLPA generally agree with the time series of the NPSH.

As shown in Figs. 2 and 3, the NPSH in 2019 is the weakest throughout the years, whereas the NPSH is even strengthened in 2020 when the Blob occurs. Thus, it is interesting to compare the net surface heat fluxes and highlight the different roles atmospheric forcing played in the two Blob events. In Fig. 4a and c, the longwave radiation and turbulent heat flux exhibit net cooling effects in the 2019 summer, while the net shortwave radiation heats the ocean significantly. The regressions between the

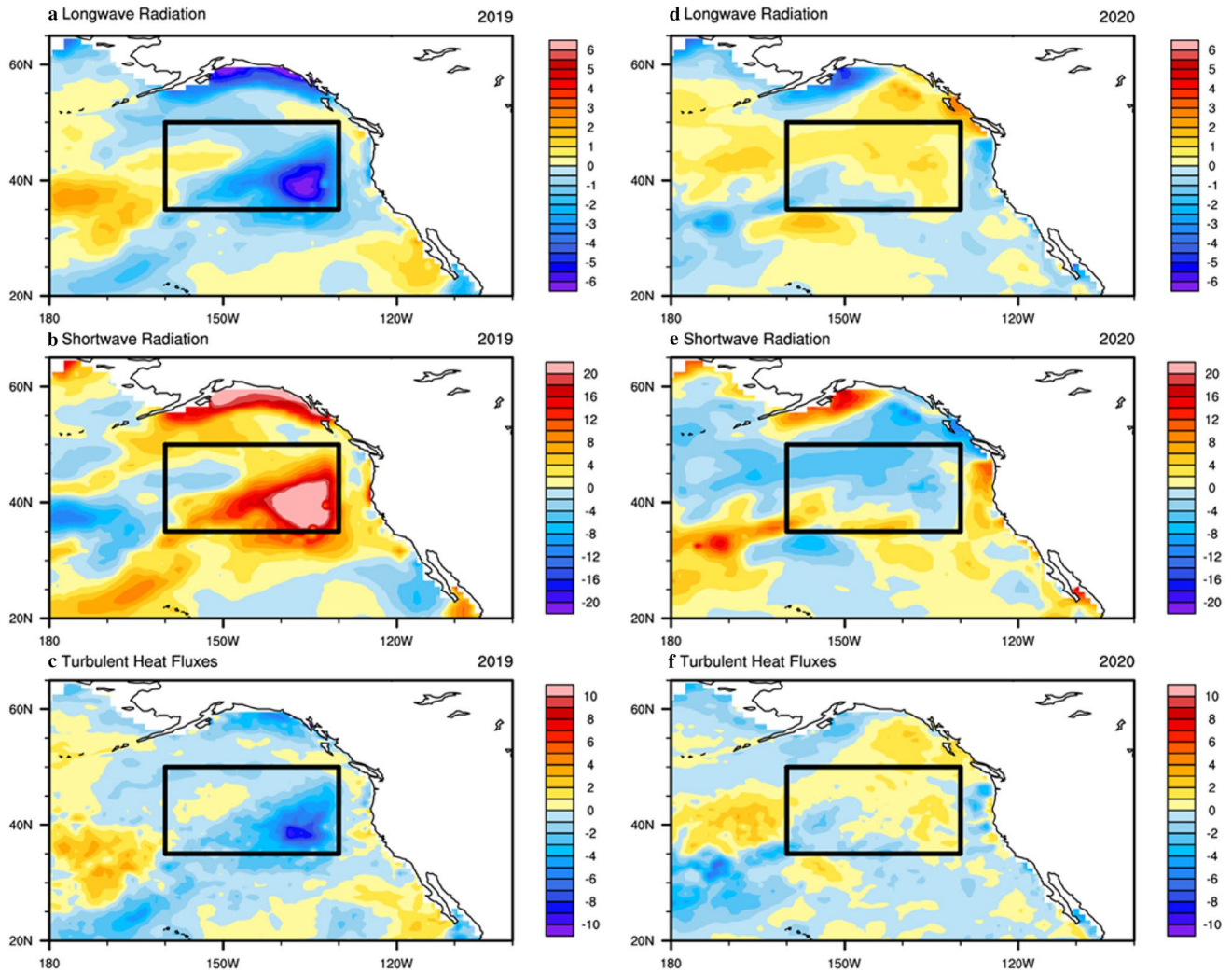

Fig. 4 **a–c** Are the anomalies of the surface longwave radiation ($W \cdot m^{-2}$), shortwave radiation, and turbulent heat flux in the summer of 2019, while **d–f** are in the summer of 2020. The positive sign indicates net heat flux into the ocean

heat fluxes and the NPSH are also examined (not shown here), and the patterns are generally consistent with those in 2019. The NPSH shifts northward during the boreal summer (Choi et al. 2016; Schmidt and Grise 2019), with low-level clouds generated in the North Pacific. As the weakening of the NPSH is observed in the North Pacific, the low-level cloud fraction is significantly reduced, which intensifies the downward shortwave radiation that induces the SST warming (Fig. 4b). The SST warming further suppresses the low-level cloud and reinforces the warm anomaly, referred to as SST-low-level cloud positive feedback (Clement et al. 2009). This is consistent with the previous studies (Amaya et al. 2020; Schmeisser et al. 2019). We also examine the heat flux anomalies in the summer of 2020 (Fig. 4d and f). The surface radiative heat flux indicates a heat loss from the ocean due to significantly reduced shortwave radiation. Meanwhile, there is weak but positive longwave radiation into the ocean, implying an increased cloud fraction. It is not surprising, considering that the NPSH is actually strengthened in 2020, which indicates an opposite atmospheric forcing.

We then inspect the mixed layer heat flux anomalies in 2014 and 2015 averaged over the Blob region and compare them with those in 2019 and 2020 (Fig. 5). Each term of heat flux is computed considering the mixed layer perturbation effect and the shortwave penetration. For the turbulent heat flux, it exhibits a cooling effect, or it is too weak to induce substantial SST warming during the four Blobs. For the shortwave radiation, it is considerably strong in 2019 that agrees with the SST-low-level cloud positive feedback in response to the weakened NPSH, whereas it shows a significant cooling effect in 2020, consistent with the spatial

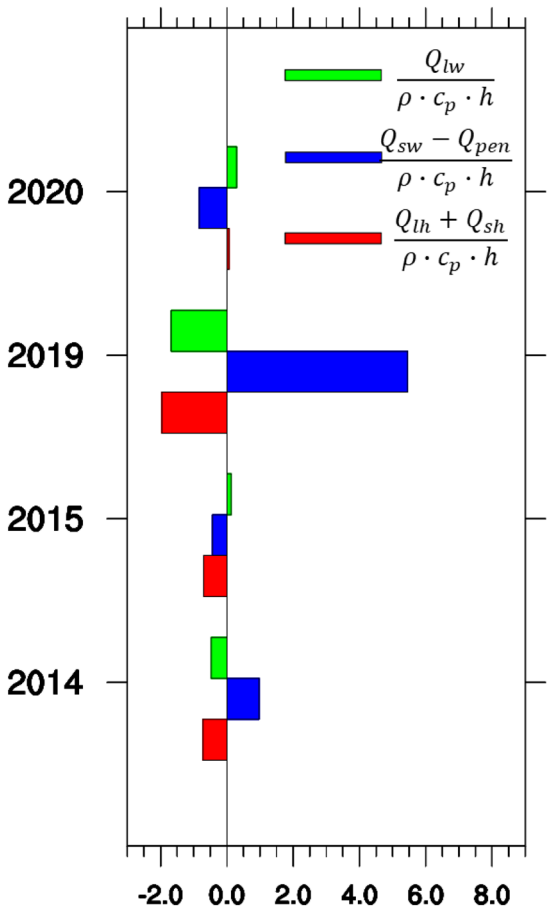

Fig. 5 The summer mixed layer heat flux components in 2014, 2015, 2019, and 2020 (longwave radiation, green bars; shortwave radiation, blue bars; turbulent heat flux, red bars) contributing to temperature changes (unit: K). Terms are calculated by the equations indicated above, using monthly heat fluxes data from ERA5. It has been multiplied by three months to gain the seasonal temperature changes from each term

patterns (Fig. 4). As the intensities of the NPSH are close to the climatology, the heat fluxes are relatively weak compared to those in 2019. The shortwave radiation cools (heats) the ocean in 2015 (2014), corresponding to the high (low) SLP anomalies in the northeast Pacific. Based on the above analysis, the atmospheric forcing associated with the NPSH cannot exclusively explain all Blob events. In 2014, 2015, and 2020, the warm anomalies developed with the absence of a strongly weakened NPSH and the corresponded intense shortwave heating (like in 2019), indicating that the formation of summer Blob indeed has diversity and the NPSH is not the only factor.

3.2 Mixed layer heat budget analysis

To take a deeper look at what causes the SST warming during the Blobs, we further conduct a mixed layer heat budget analysis for the period 1982–2020. As shown in Fig. 6, the mixed layer temperature in the northeast Pacific is mainly balanced by the warming effect caused by total surface heat flux and the cooling effect associated with the entrainment in the bottom of the mixed layer. The advective term is rather weak (about one order smaller than the other terms), considering the large volume of the mixed layer and relatively weak eddy kinetic energy in the northeast Pacific (Amaya et al. 2020; Qiu 2002). Both horizontal and vertical advection have slight warming effects, but the total contribution to the SST warming is minor, suggesting that the influence of non-local effect associated with advection to the summer Blob is limited.

As shown in Fig. 6, the total heat flux is a primary heating term, which represents the intensity of atmospheric forcing imposed on the mixed layer. The correlation coefficient between the JJA total heat flux and the Blob can reach 0.40, which reveals a close instantaneous connection between the

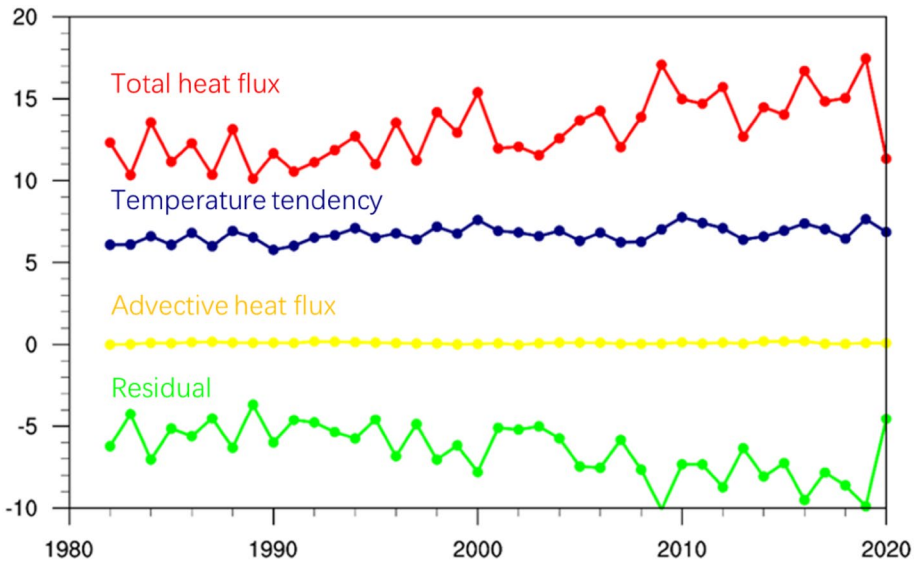

Fig. 6 The temperature tendency (blue; unit: K) derived from the difference between the August and May SSTA and the respective budget terms (unit: K) contributing to the temperature changes, which include the components from adjusted total heat flux (red), advective heat flux (yellow), and residual (green). The total heat flux and ocean current data are derived from the NCEP GODAS reanalysis for the period 1982–2020

Blob and atmospheric forcing. In contrast, the lagged influence of MAM heat flux may be limited to the following season's warm SSTA (r = 0.09) (supplementary Fig. 1). The JJA total heat flux reaches the highest in 2019 and lowest in 2020, consistently indicating contrasting roles that the atmospheric forcing played between the two Blob events. It is also worth noting that the total heat fluxes in 2014 and 2015 that correspond with the slightly weakened NPSH show no prominent heating, further indicating that the contemporary atmospheric forcing is too weak to sustain the SST warm anomalies during the summer.

In addition to the surface radiative heat flux (Q_{net}) associated directly with the weakened NPSH, the total heat flux ($\frac{Q_{net}-Q_{pen}}{\rho c_p h_m}$) term is also influenced by the mixed layer depth (h_m). Here, the time series of the JJA mixed layer depth over the northeastern Pacific is further inspected (supplementary Fig. 2). The mixed layer exhibits a significant shoaling trend over the analyzed period, corresponding well with the reduced wind stress over the northeast Pacific. The temperature in a shallower mixed layer more efficiently responds to the inlet heat flux, which leads to more intense SST warming in response to the atmospheric forcing. This further enhances the SST-cloud-shortwave radiation feedback, which is consistently indicated by a decreasing trend in low-level cloud cover shown in a previous study (Amaya et al. 2020), corresponding to a long-term increasing trend in the total heat flux. Since more heat could be retained and concentrated within a shallower mixed layer, it would represent a stronger atmospheric forcing on the Blob event, such as the one in 2019. Therefore, the intensity of atmospheric forcing similar to the past may be more efficient in inducing a Blob event than the previous due to the shoaling mixed layer. In supplementary Fig. 2, we also find that the vertical temperature difference (below minus above the thermocline) shares a consistent decreasing trend and is significantly correlated with the mixed layer depth (r = 0.80). As heat is trapped in a shallow mixed layer, the vertical temperature profile exhibits a sharp decline, which would influence the entrainment cooling with enlarged vertical gradients.

We also compute the temperature tendency by subtracting the monthly mean SSTA in May from the August mean SSTA, indicating the increment of SSTA during the summer (Amaya et al. 2020). It is also used to identify the timing of the warming process related to the Blob. For instance, the tendency term in 2019 is greater than in the other years, indicating that the high SSTA is likely associated with significant warming during the summer. This is consistent with the above analysis that the weakened NPSH (atmospheric forcing) induces SST warming may through the instantaneous SST-cloud-shortwave radiation feedback. As soon as the positive feedback is initiated, the shortwave radiation will heat the underlying ocean, resulting in a large increment of SSTA. The correlation coefficient between the JJA heat flux and tendency reaches 0.69, which further proves that the increment of summer SSTA can be largely explained by the contemporary total heat flux associated with the atmospheric forcing. However, the tendency and heat flux are both comparably small in 2020, yet the Blob occurred. The contemporary atmospheric forcing is weak, and the increment of SSTA during the summer is small, which implies that the SSTA inherited from the preceding season likely plays a role.

3.3 Role of spring SST persistence

It attracts our attention that the northeast Pacific SST signal can persist for a couple of months, as suggested in previous studies (Bulgin et al. 2020; Ding and Li 2009; Namias et al. 1988). We first inspect the characteristics of North Pacific SST persistence in the mid-high latitudes by calculating the lagged autocorrelations of northeastern Pacific SSTA in each calendar month for the following 12 months in Fig. 7. Note that the correlation coefficients larger than 0.6 could characterize the persistence (Ding and Li 2009). A previous study suggested that SST persistence is dependent on seasons (Namias et al. 1988). As shown in Fig. 7, the SSTA can persist over three months in winter, but the lagged correlation of the winter SST signal sees a quick drop in spring. Interestingly, the spring SST signal can even shed light on the SSTA after 1–2 seasons (0–6 months), indicating the strongest SST seasonal persistence. The lagged correlation coefficient of the summer SSTA drops below 0.6 soon after three months, indicating the so-called "summer persistence barrier." Above all, the SSTA initiated from April/May

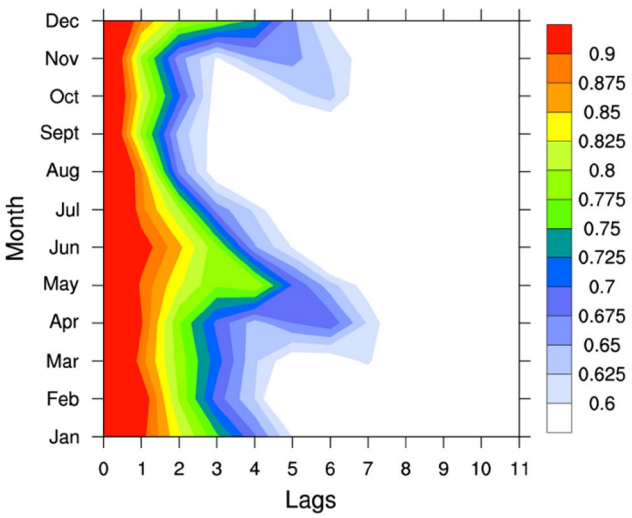

Fig. 7 Lagged correlation coefficients of the monthly northeastern Pacific SST anomalies as a function of starting calendar month and lag time (month) for the period 1982–2020

closely correlates with the SSTA during the whole summer ($r > 0.7$), whereas the contribution from the winter SSTA is comparably small, since the winter SST signal faded quickly ($r < 0.65$ after 4–5 months). The small temperature tendency, in a way, represents the contributions that persisted from the preceding SST warming signal in spring, which is significantly different from the contemporary atmospheric forcing that functions in summer.

The relationship between the summer Blob and the preceding spring (MAM mean) SSTA is analyzed to further investigate the role of SST persistence in the formation of the Blob. As shown in Fig. 8, the preceding spring SSTA and the Blob series are well corresponded, and the correlation coefficient reaches 0.79 ($r = 0.81$ detrended), indicating strong coherence between the interannual variabilities. For the Blob events in 2014, 2015, and 2020, the spring SSTs exhibit consistently prominent warm anomalies, which agrees with the spatial patterns (Fig. 9), as the maximum SST warm anomaly exceeded 1.2℃ in these years. In Fig. 7, the spring SSTA can persist over a season so that the summer Blob inherits, more or less, the spring SST warm anomalies, which is clearly seen in 2014, 2015, and 2020. However, only in 2019 the spring SSTA shows comparably weak warming over the northeastern Pacific (less than 0.4 ℃). In addition, significant warming can be found over the northern North Pacific. Therefore, we compare it with the JJA Blob index, which shows little coherence with the extreme SST warming events, suggesting that the northern North Pacific SST can be distinguished from the spring SST persistence over the northeastern Pacific. Thus, with a weak

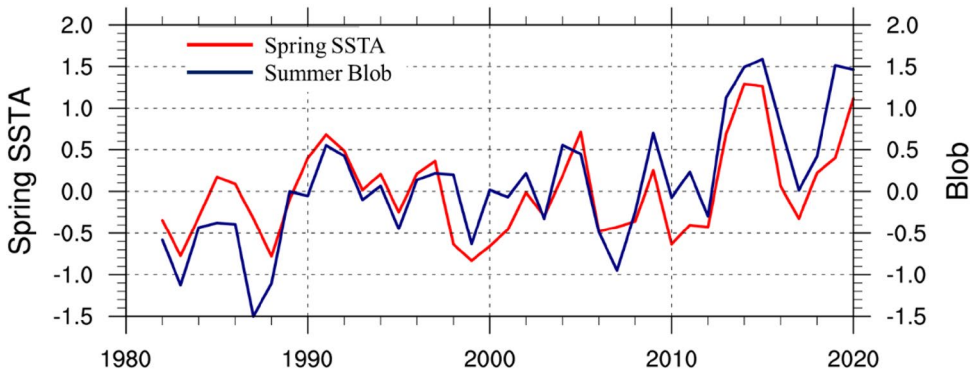

Fig. 8 The time series of the summer (JJA) Blob (blue line) and the spring (MAM) SSTA (red line) averaged over the Blob region (35°–50°N, 160°–130°W) for the period 1982–2020

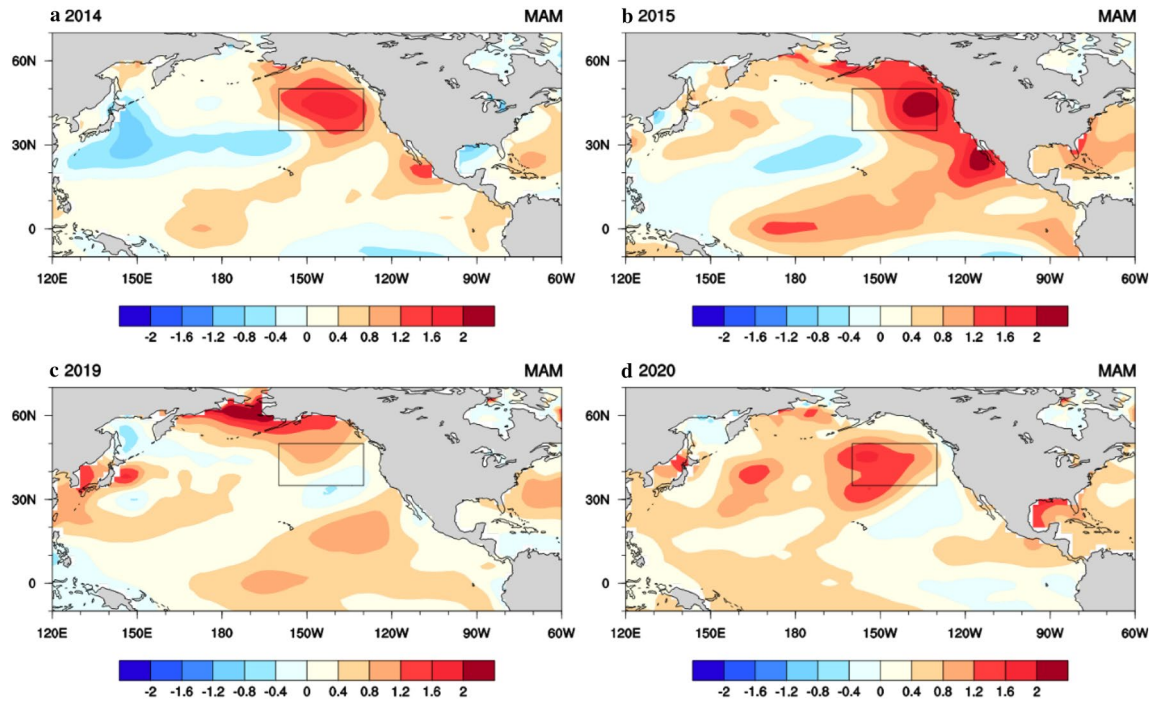

Fig. 9 The SST anomalies (K) in the spring (MAM mean) of (**a**) 2014, (**b**) 2015, (**c**) 2019, (**d**) 2020. The black box indicates the location of the summer Blob (35°–50°N, 160°–130°W).

SST anomaly in the preceding spring, the SST persistence seemed not applicable for the Blob in 2019.

The above results further highlight the diversity in the summer Blobs. For the origin of spring SST persistence, here we calculate the mixed layer heat content anomaly during the preceding spring (Fig. 10). During the four Blob events, the ocean heat content is anomalously large in 2014, 2015, and 2020, which is over two times higher than that in 2019. More heat content in the mixed layer indicates the warm anomaly could decay slower and have a long-lasting influence in the following seasons, exhibiting an SST persistence. We can find that the persistent SST warming signal also is stronger in 2014, 2015, and 2020, consistent with the heat content anomaly.

However, even with large heat content and strong SST persistence, the spring SST should have decayed from spring to summer without contemporary heat sources, but this would disagree with the positive temperature tendency when the SST persistence dominates the Blob. Here we find that the anomalous entrainment cooling in the bottom of the mixed layer may reconcile the discrepancy. As shown in Fig. 6, the entrainment mainly exhibits a net cooling effect balanced by the surface heat fluxes warming related to the atmospheric forcing. It is noticeable that the intensity of entrainment cooling shows significant differences among the Blob events. The anomalously weak entrainment during the Blob (such as in 2014, 2015, and 2020) prohibits the cooler deep water from entering the mixed layer, reducing the cooling effect. Thus, the warm anomaly can be easily retained in the mixed layer and favors the summer Blob.

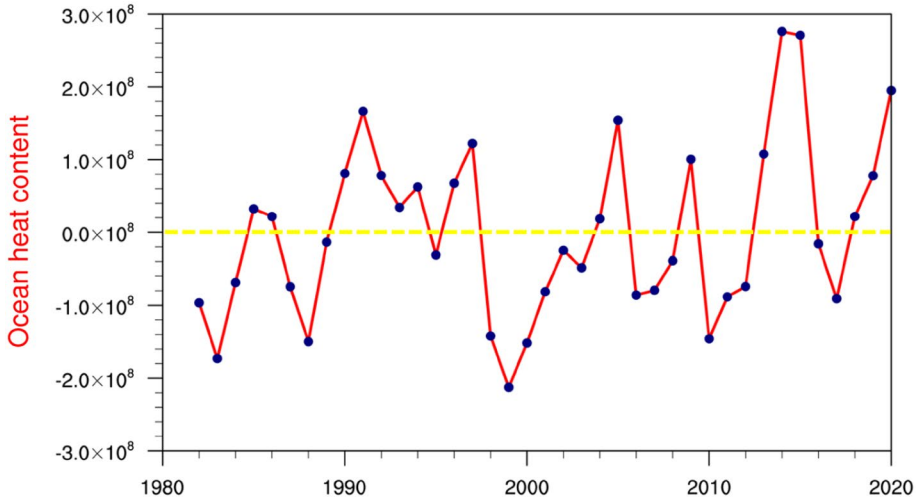

Fig. 10 The anomalies of mixed layer heat content ($J{\cdot}m^{-2}$) in spring (MAM mean) over the Blob region. The series is analyzed for the period 1982–2020

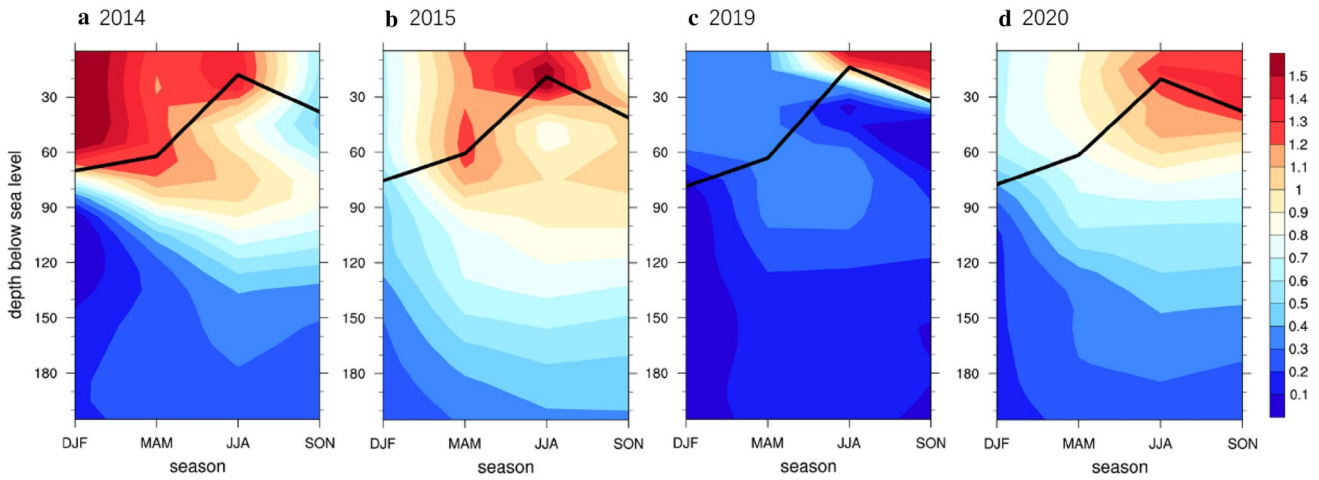

Fig. 11 The subsurface structure (0–210 m) in the northeast Pacific, which includes temperature anomalies (contour; unit: K) and mixed layer depth (solid line; unit: m) over four seasons (D(− 1)JF, MAM, JJA, and SON) in **a** 2014, **b** 2015, **c** 2019, and **d** 2020

3.4 Subsurface structure of Blob

We further analyze the subsurface structure of the Blob event in 2014, 2015, 2019, and 2020 using the GODAS ocean reanalysis (Fig. 11). The temperature anomaly and mixed layer depth data are averaged over the Blob region, and the seasonal means of winter (DJF), spring (MAM), summer (JJA), and autumn (SON) are derived to depict the evolution. There are noticeable differences in temperature anomalies prior to the summer when the Blob occurs. In the winter of 2014, it was recorded an unprecedented Blob event (Bond et al. 2015; Di Lorenzo and Mantua 2016). However, the warm anomaly quickly withdrew from winter to spring, which is also consistent with that shown in Fig. 7, and the warming signal transmits equatorward in the following seasons via the wind-evaporation-SST (WES) feedback (Di Lorenzo and Mantua 2016; Tseng et al. 2017). Nevertheless, the warm-than-normal mixed layer condition prior to the Blob is able to persist till summer and significantly contribute to the extremes. Aside from the extreme situation in the winter of 2014, the mixed layer in 2015 was also warmer-than-normal in the spring. A warm core is found at the bottom of the mixed layer with a temperature anomaly exceeding 1.2 degrees. In addition, the temperature well below the mixed layer is also warmer. The near-surface temperature exhibits significant persistence from spring to summer. The subsurface structure in 2020 is similar to that in 2015. The temperatures within and below the mixed layer are anomalously warm in spring. The mixed layer temperature anomaly can reach 1.0 degrees prior to the Blob. Based on the above analysis, the preceding spring mixed layer temperatures in 2014, 2015, and 2020 are anomalously warm to some extent, and the near-surface warming persists into the following summer, which may contribute to the Blob. It is clear that the mixed layer heat contents prior to the Blob are higher than normal, which explains the origin of SST warming persistence (Fig. 10). On the other hand, the subsurface structure of the northeast Pacific in 2019 is quite different. The entire mixed layer temperature prior to the Blob is far less warmed, with the anomaly below 0.4 K. It corresponds well with the mixed layer temperature tendency in Fig. 6. Moreover, the mixed layer heat content in the spring of 2019 is also small due to a much cooler mixed layer temperature, indicating that the persistence of preceding SST warming is considerably weak in 2019.

3.5 A binary linear regression model for the blob

In this study, we find that both contemporary atmospheric forcing (the NPSH) and the preceding oceanic forcing (SST persistence) are responsible for the summer Blob. The partial correlation coefficient between the NPSH and summer Blob without the influence of spring SSTA remains around 0.3, indicating that the NPSH-Blob relationship is unlikely dominated by the spring SST persistence. The physical processes associated with these two factors are also significantly different. One is related to the SST-cloud-shortwave radiation feedback, while the other is related to the anomalous mixed layer heat content prior to the Blob. Thus, these two factors and the associated mechanisms are independent of one another. Further, we can construct a binary linear regression model that synthetically considers the forcing roles of summer NPSH and spring SST persistence. It is shown as follows:

$$Blob_{summer}(t) = a \cdot SST_{spring}(t) + b \cdot NPSH_{summer}(t)$$

where a, and b are coefficients and t is year. $SST_{spring}(t)$ and $NPSH_{summer}(t)$ indicate the effects of preceding SST persistence and simultaneous atmospheric forcing, respectively.

In Fig. 12, the modeled series that considers the mechanisms learned from the four case studies is able to reproduce the observed interannual variability in the northeast Pacific (r = 0.76). The results are still robust without the warming trend (r = 0.77), further suggesting that the mechanisms found in the four cases are independent of the long-term trend. Note that the regression model based solely on the spring SST can overall reproduces the interannual variability three months in advance, showing its potential in predicting the Blob events. However, the SST-based model also exhibits considerable biases compared to observation. It indicates that only taking the spring SSTA into account may lead to significant underestimation during some peak years. Therefore, it is necessary to take both factors into account so that the model can reproduce the interannual SST variability over the northeastern Pacific but also capture the extreme

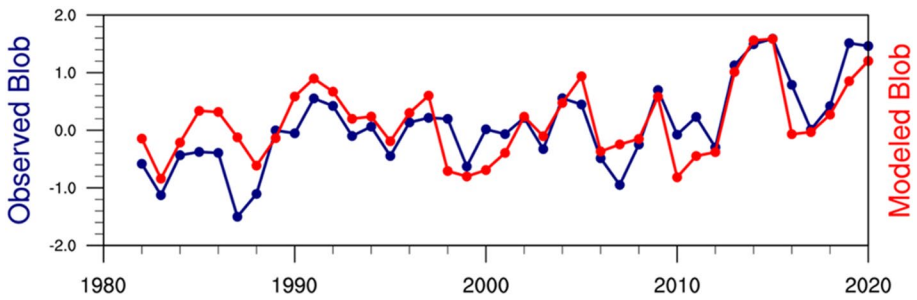

Fig. 12 The time series of observed summer (JJA mean) Blob (blue line) and the modeled Blob (red line) from the binary linear regression model with two factors involved (the NPSH and the spring SSTA; see main text for the equation and details) for the period 1982–2020

Blob events. The binary linear regression model provides additional evidence that the summer Blob has diversity in its formation associated with both the atmospheric forcing and the SST persistence.

Previous studies have revealed a connection between the winter Blob events and ENSO/PDO. The correlation coefficient between the summer Blob and Nino 3.4 (EP- El Niño) only reaches 0.23. The strong Blob and EP- El Niño events are barely matched (not shown here). In addition, we also compare the SST regression pattern of the reconstructed Blob series with the observed one. The residual, although small, resembles the PDO pattern to some extent. We then inspect the relationship between the detrended Blob and PDO indices. The correlation coefficient between them is −0.13 (detrended). The interannual variability of the Blob is somewhat coherent with that of the PDO, but the extremes generally do not correspond. Therefore, the influences of EP- El Niño and PDO on the formation of summer Blob may be limited.

4 Conclusion and discussion

The NPSH is regarded as a common forcing regulating the northeast Pacific SST variability through anomalous heat fluxes associated with the SST-cloud positive feedback (Amaya et al. 2020). In this study, we identified four recent Blob events during the summer, some of which are related to the weakened NPSH, and it is most significant during the 2019 Blob event. In addition to the atmospheric forcing, we find that the persistence of spring SST warming, associated with large mixed layer heat content, also favors the formation of Blob. The prohibited cooling at the bottom of the mixed layer may help sustain the warm anomaly from spring to summer and contributes to its persistence. A multiple linear regression model considering both the NPSH and spring SSTA successfully reproduces the observed Blob series and improves the ability to capture the warm peaks, which neither single factor can fully depict. Our results provide evidence that the formation of summer Blob has diversity.

In this study, we also find that the relationship between the NPSH and the Blob has strengthened in recent decades, as the 15-year running correlation coefficients have substantially increased to around −0.35 since 1989 (supplementary Fig. 3a). We then examine the correlation map between the NPSH and tropical SSTA, which exhibits significant tropical Central Pacific warming that resembles the CP-El Niño pattern since 1989 (supplementary Fig. 3b). Previous studies have indicated the shifts from EP-El Niño to CP-El Niño (Yeh et al. 2009, 2011) around 1990. The increased occurrence of CP-El Niño may be responsible for the strengthened relationship between the NPSH and the Blob. The low-frequency variation of Blob and its relation with tropical SST may need further investigation. In addition to internal variability, the spring and summer SST over North Pacific consistently exhibits a long-term warming trend, as shown in Fig. 8. The warming background may also play a role, as the mean state warming corresponds well with the increased extreme events. Therefore, the relationship between external forcing and the recent changes in Blob warrants further investigations.

Supplementary Information The online version contains supplementary material available at https://doi.org/10.1007/s00382-022-06584-8.

Acknowledgements Not Applicable.

Author contributions CS, designed the research. YL, and CS, performed the data analysis, prepared all figures and led the writing of the manuscript. All the authors discussed the results and commented on the manuscript.

Funding This work is jointly supported by the National Natural Science Foundation of China (41790474, and 41975082) and Shandong Natural Science Foundation Project (ZR2019ZD12).

Data availability The datasets generated during and/or analyzed during the current study are available to the public. Detailed information has been provided in the "Data and Method" section in the manuscript.

Declarations

Conflict of interest The authors have no relevant financial or non-financial interests to disclose.

Ethical approval and consent to participate Not Applicable.

Consent for publication Not Applicable.

References

Alexander MA, Deser C, Timlin MS (1999) The reemergence of SST anomalies in the North Pacific Ocean. J Clim 12:2419–2433

Amaya D, Bond N, Miller A, DeFlorio M (2016) The evolution and known atmospheric forcing mechanisms behind the 2013–2015 North Pacific warm anomalies. US Clivar Var 14:1–6

Amaya DJ, Miller AJ, Xie S-P, Kosaka Y (2020) Physical drivers of the summer 2019 North Pacific marine heatwave. Nat Commun 11:1–9

Amaya DJ, Alexander MA, Capotondi A, Deser C, Karnauskas KB, Miller AJ, Mantua NJ (2021) Are long-term changes in mixed layer depth influencing North Pacific marine heatwaves? Bull Am Meteorol Soc 102:S59–S66

An S-I, Wang B (2005) The forced and intrinsic low-frequency modes in the North Pacific. J Clim 18:876–885

Behringer D, Xue Y (2004) Evaluation of the global ocean data assimilation system at NCEP: the Pacific ocean. In: Proc. eighth symp. on tntegrated observing and assimilation systems for atmosphere, aceans, and land surface,

Bond NA, Cronin MF, Freeland H, Mantua N (2015) Causes and impacts of the 2014 warm anomaly in the NE Pacific. Geophys Res Lett 42:3414–3420

Bulgin CE, Merchant CJ, Ferreira D (2020) Tendencies, variability and persistence of sea surface temperature anomalies. Sci Rep 10:1–13
Chen Z, Shi J, Liu Q, Chen H, Li C (2021) A persistent and intense marine heatwave in the Northeast Pacific during 2019–2020. Geophys Res Lett 48:e2021GL093239
Choi J, Lu J, Son SW, Frierson DMW, Yoon JH (2016) Uncertainty in future projections of the North Pacific subtropical high and its implication for California winter precipitation change. J Geophys Res Atmos 121:795–806. https://doi.org/10.1002/2015jd023858
Clement AC, Burgman R, Norris JR (2009) Observational and model evidence for positive low-level. Cloud Feedback Science 325:460–464. https://doi.org/10.1126/science.1171255
Deser C, Alexander MA, Timlin MS (2003) Understanding the persistence of sea surface temperature anomalies in midlatitudes. J Clim 16:57–72
Di Lorenzo E, Mantua N (2016) Multi-year persistence of the 2014/15 North Pacific marine heatwave. Nat Clim Change 6:1042–1047
Ding R, Li J (2009) Decadal and seasonal dependence of North Pacific sea surface temperature persistence. J Geophys Res Atmos 114:D01105
Hartmann DL (2015) Pacific sea surface temperature and the winter of 2014. Geophys Res Lett 42:1894–1902
Hersbach H et al (2020) The ERA5 global reanalysis quarterly. J Royal Meteorol Soc 146:1999–2049
Huang B et al (2017) NOAA extended reconstructed sea surface temperature (ERSST), version 5 NOAA National. Cent Environ Inf 30:8179–8205
Kanamitsu M, Ebisuzaki W, Woollen J, Yang S-K, Hnilo J, Fiorino M, Potter G (2002) Ncep–doe amip-ii reanalysis (r-2). Bull Am Meteorol Soc 83:1631–1644
Lee S-B, Yeh S-W, Lee J-S, Park YG, Kwon MH, Jun S-Y, Jo H-S (2022) Roles of atmosphere thermodynamic and ocean dynamic processes on the upward trend of summer marine heatwaves occurrence in East Asian marginal seas. Front Marine Sci 9:889500
Liu Y, Sun C, Kucharski F, Li J, Wang C, Ding R (2021) The North Pacific Blob acts to increase the predictability of the Atlantic warm pool. Environ Res Lett 16:064034
Namias J, Born RM (1970) Temporal coherence in North Pacific sea-surface temperature patterns. J Phys Res 75:5952–5955
Namias J, Yuan X, Cayan DR (1988) Persistence of North Pacific sea surface temperature and atmospheric flow patterns. J Clim 1:682–703
Paulson CA, Simpson JJ (1977) Irradiance measurements in the upper ocean. J Phys Oceanogr 7:952–956
Peterson WT, Fisher JL, Strub PT, Du X, Risien C, Peterson J, Shaw CT (2017) The pelagic ecosystem in the Northern California current off Oregon during the 2014–2016 warm anomalies within the context of the past 20 years. J Geophys Research: Oceans 122:7267–7290
Qiu B (2002) The Kuroshio Extension system: Its large-scale variability and role in the midlatitude ocean-atmosphere interaction. J Oceanogr 58:57–75
Rodionov SN (2004) A sequential algorithm for testing climate regime shifts. Geophys Res Lett 31(9):L09204
Scannell HA, Johnson GC, Thompson L, Lyman JM, Riser SC (2020) Subsurface evolution and persistence of marine heatwaves in the Northeast Pacific. Geophys Res Lett 47:e2020GL090548
Schmeisser L, Bond NA, Siedlecki SA, Ackerman TP (2019) The role of clouds and surface heat fluxes in the maintenance of the 2013–2016 Northeast Pacific marine heatwave. J Geophys Res Atmos 124:10772–10783. https://doi.org/10.1029/2019jd030780
Schmidt DF, Grise KM (2019) Impacts of subtropical highs on summertime precipitation in North America. J Geophys Res Atmos 124:11188–11204. https://doi.org/10.1029/2019jd031282
Seager R et al (2015) Causes of the 2011–14 California drought. J Clim 28:6997–7024
Shi H, García-Reyes M, Jacox MG, Rykaczewski RR, Black BA, Bograd SJ, Sydeman WJ (2021) Co-occurrence of California drought and Northeast Pacific marine heatwaves under climate change. Geophys Res Lett 48:e2021GL092765
Tak Y-J, Song H, Cho Y-K (2021) Impact of the reemergence of North Pacific subtropical mode water on the multi-year modulation of marine heatwaves in the North Pacific ocean during winter and early spring. Environ Res Lett 16:074036
Tseng Y-H, Ding R, Huang X-m (2017) The warm Blob in the northeast Pacific—the bridge leading to the 2015/16 El Niño. Environ Res Lett 12:054019
Wernberg T et al (2016) Climate-driven regime shift of a temperate. Mar Ecosyst Sci 353:169–172. doi:https://doi.org/10.1126/science.aad8745
Xu T, Newman M, Capotondi A, Di Lorenzo E (2021) The continuum of Northeast Pacific marine heatwaves and their relationship to the tropical Pacific. Geophys Res Lett 48:2020GL090661
Yeh S-W, Kug J-S, Dewitte B, Kwon M-H, Kirtman BP, Jin F-F (2009) El Niño in a changing climate. Nature 461:511–514
Yeh SW, Kirtman BP, Kug JS, Park W, Latif M (2011) Natural variability of the central Pacific El Niño event on multi-centennial timescales. Geophys Res Lett. 38: L02704. https://doi.org/10.1029/2010GL045886
Yun KS, Yeh SW, Ha KJ (2013) Distinct impact of tropical SSTs on summer North Pacific high and western North Pacific subtropical high. J Geophys Res Atmos 118:4107–4116
Zhou X, Marsland SJ, Fiedler R, Bi D, Hirst AC, Alves O (2015) Impact of different solar penetration depths on climate simulations. Tellus A Dyn Meteorol Oceanogr 67:25313